
LaVi: Efficient Large Vision-Language Models via Internal Feature Modulation

Tongtian Yue^{1,2*}, Longteng Guo^{1,2*}, Yepeng Tang^{3*},
Zijia Zhao^{1,2}, Xinxin Zhu^{1,2}, Hua Huang⁴, Jing Liu^{1,2†}

¹Institute of Automation, Chinese Academy of Sciences

²School of Artificial Intelligence, University of Chinese Academy of Sciences

³Institute of Information Science, Beijing Jiaotong University

⁴School of Artificial Intelligence, Beijing Normal University

Abstract

Despite the impressive advancements of Large Vision-Language Models (LVLMs), existing approaches suffer from a fundamental bottleneck: inefficient visual-language integration. Current methods either disrupt the model’s inherent structure or introduce severe long-context computational burden, severely limiting scalability and efficiency. In this paper, we rethink multimodal integration and present LaVi, a novel LVLM that enables seamless and efficient vision-language fusion through internal feature modulation within the Large Language Models (LLMs). Unlike dominant LVLMs that rely on visual token concatenation, LaVi bypasses long-context expansion by introducing a lightweight and adaptive transformation, which incorporates visual context by injecting token-wise vision-conditioned *deltas* into the affine parameters of layer normalization. This mechanism directly modulates linguistic hidden states based on visual input, ensuring precise vision-language alignment while preserving the LLM’s linguistic priors and drastically reducing computational costs. Extensive evaluations across 15 image and video benchmarks demonstrate that LaVi not only achieves state-of-the-art multimodal performance but also dramatically enhances efficiency. Compared to LLaVA-OV-7B, LaVi reduces FLOPs by 94.0%, improves inference speed by 3.1×, and cuts memory usage in half — establishing LaVi as a scalable and practical solution for real-time multimodal reasoning. The code and models will be released soon.

1 Introduction

Recently, significant advancements in Large Language Models (LLMs) [50, 1, 63, 58] have catalyzed the emergence of Large Vision-Language Models (LVLMs) [8, 39, 6, 57], demonstrating remarkable capabilities in visual perception and cognitive reasoning [42, 19, 53, 25]. While considerable progress has been achieved separately in visual encoding and language generation, the pivotal challenge of effectively integrating visual information into LLMs still remains open.

Existing integration techniques generally fall into two categories. The first, termed *architectural injection* (e.g., Flamingo [6]), augments the original LLMs by introducing additional layers [2, 48, 64], such as cross-attention and feed-forward layers, strategically throughout the model. While these modules explicitly insert visual features into the linguistic processing pathway, their introduction inherently disrupts the architectural coherence and processing flow of the original LLMs. Consequently, it can degrade the delicate pre-trained language understanding, risking losing the rich linguistic priors encoded within LLMs [72, 45, 62]. The second and currently predominant approach, *in-context injection* (e.g., the LLaVA series [40, 39, 27]), integrates visual information by concatenating vision-derived token sequences directly into textual input, treating them as part of the initial context for

*Equal Contribution.

†Corresponding author.

the LLMs. While preserving architectural integrity, this method introduces significant practical challenges. Specifically, the large number of visual tokens required (*e.g.*, 576 tokens for a single image using CLIP ViT-L/336px [49]) leads to severe computational overhead due to the quadratic complexity inherent in self-attention mechanisms [60]. This complexity escalates dramatically when processing high-resolution images or long video sequences, resulting in substantial inference latency and computational bottlenecks, thus hindering real-time applicability.

Through analyzing these methods, we argue that an ideal visual-language integration strategy must satisfy two fundamental principles: 1) *minimal structural interference*, which ensures the preservation of pretrained linguistic knowledge to support coherent text generation and empower vision-grounded understanding and reasoning; and 2) *computational scalability*, which mitigates inefficiencies arising from quadratic complexity when processing extensive visual tokens.

Guided by these principles, we propose a new visual-language integration strategy for LVLMs: internal *Feature Modulation Injection* (FMI) within the LLMs. Central to FMI is the layer normalization (LN) mechanism [7, 68], a ubiquitous component in modern LLMs. LN applies learnable affine transformations to rescale and shift the features, offering a natural pathway for updating the internal hidden states through a combination of additive and multiplicative modulation. Inspired by this, we introduce Vision-Infused Layer Normalization (ViLN), a lightweight yet effective extension of standard LN that integrates visual context into language modeling. Specifically, ViLN dynamically adjusts the affine transformation parameters of LN via vision-conditioned *deltas*, thereby enabling visual signals to modulate token-wise linguistic representations in a fine-grained and context-aware manner. Based on ViLN, FMI provides notable advantages by minimally intervening within the pretrained LLM, thus preserving its linguistic priors and relieving the impact on linguistic performance. Moreover, by avoiding direct incorporation of visual tokens into self-attention, our method circumvents the quadratic complexity issue, achieving superior computational scalability and efficiently accommodating extensive visual data such as high-resolution images and long videos.

Building upon this strategy, we present **LaVi** (Language and Vision Integrator), a novel LVLm that seamlessly incorporates FMI through selective replacement of standard LN layers with ViLN modules. To supply ViLN with the necessary visual conditions, LaVi employs a conditioning module that generates a dedicated visual condition for each text token, allowing token-wise modulation informed by the visual features. The design of this conditioning module is highly flexible, and we explore three alternative implementations: MLP-based, convolution-based, and attention-based approaches, each offering a favorable trade-off between computational efficiency and multimodal performance. Once the visual conditions are obtained, each is transformed into vision *deltas* of the affine parameters through a lightweight learnable mapping, which are then used to modulate the corresponding linguistic features within the LLM.

Benefiting from a significantly reduced context length and a lightweight yet effective visual-language integration strategy, LaVi strikes an impressive balance between computational efficiency and benchmark performance. Comprehensive evaluations across 9 image-based and 6 video-based understanding benchmarks demonstrate that LaVi achieves state-of-the-art performance comparable to LLaVA-style models while substantially reducing computational overhead. Moreover, it maintains superior linguistic capabilities compared to using other injection strategies. Compared to the baseline LLaVA-OV-7B [27], LaVi, despite maintaining the same 7B parameter scale, demonstrates substantial improvements in both efficiency and performance. It achieves an impressive 94.0% reduction in FLOPs, operates 3.1x faster, lowers memory

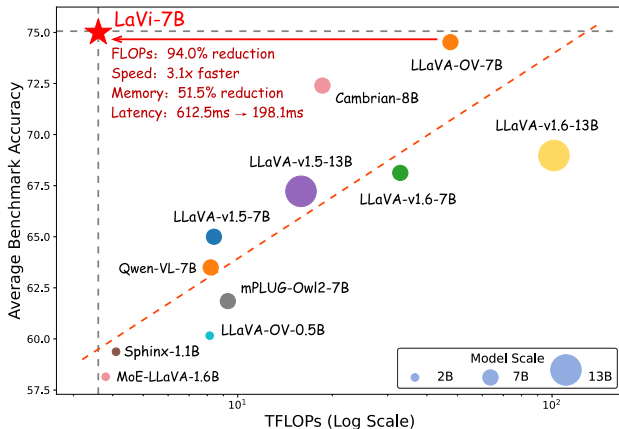


Figure 1: **Comparison between LaVi and open-source LVLms on image understanding benchmarks.** We report the average accuracy on MMBench [42], MME [19], TextVQA [53], and GQA [25]. For MME, scores are normalized to percentages. The red dashed line represents the linear fit to all models except LaVi.

consumption by 51.5%, and reduces inference latency from 612.5 ms to just 198.1 ms, as illustrated in Figure 1. Remarkably, LaVi requires even fewer FLOPs than LLaVA-OV-0.5B [27], yet surpasses it by +15.5 points in benchmark accuracy. These advancements significantly enhance real-time multimodal interactions, positioning LaVi as a highly efficient alternative in the evolving landscape of LVLMs.

Our contribution can be concluded as:

- We introduce a novel internal feature modulation injection paradigm for LVLMs. It ensures minimal structural interference, effectively preserves pretrained linguistic priors, and achieves computational scalability by avoiding excessive context length expansion.
- We propose LaVi, a highly efficient LVLM capable of comprehensive image and video understanding. LaVi integrates ViLN to achieve fine-grained visual-linguistic alignment and investigates various visual conditioning mechanisms, effectively balancing multimodal performance with computational efficiency.
- LaVi achieves state-of-the-art performance across multimodal benchmarks while significantly improving computational efficiency. Compared to the LLaVA-style baseline, LaVi reduces FLOPs by 94.0%, offering an efficient and practical solution for real-time multimodal processing with significantly reduced resource demands.

2 Related Work

Large Vision-Language Models.

Large Vision-Language Models (LVLMs) have significantly advanced multimodal understanding, enabling more effective integration of vision and language. Closed-source models such as Claude [4], GPT [1], and Gemini [55] series exhibit strong multimodal capabilities. Meanwhile, open-source models like LLaVA [41, 39, 40, 27], BLIP [30, 29], Qwen-VL [8, 63], and InternVL [15, 14] series have contributed significantly to the community by providing accessible and adaptable alternatives. Recent research has focused on improving input resolution [40, 22], enhancing training and inference efficiency [11, 61], and extending multimodal capabilities to temporal video sequences [32, 69, 46]. These advancements continue to push the boundaries of LVLMs in efficiency, scalability, and multimodal reasoning.

Multimodal Integration. Multimodal integration, which aims to effectively fuse visual and language representations, is a fundamental challenge in multimodal learning. A common approach is to directly concatenate or perform element-wise operations (*e.g.*, addition or multiplication) on vision and language features, which has been widely adopted in tasks such as visual question answering (VQA) [5, 26] and vision-language representation learning [13, 43]. In the LVLM domain, LLaVA [41] also employs this straightforward method, inspiring many subsequent works. While this approach is computationally simple, it significantly increases sequence length, posing efficiency challenges. An alternative strategy involves using additional fusion structures, such as cross-attention mechanisms [3, 66] or multi-layer transformers [30, 31], which introduce learnable parameters to compress multimodal representations more effectively. However, such modifications (*e.g.*, Flamingo [6]) can disrupt the pretrained data flow of the underlying LLM, potentially degrading language capabilities or increasing complexity.

3 Methodology

3.1 Preliminaries

In this section, we begin with a concise overview of the predominant visual-language integration strategies employed in LVLMs. Specifically, existing methods primarily fall into two categories: architectural injection and in-context injection:

Architectural Injection. As illustrated in Figure 2a, this approach integrates visual information by inserting additional interaction layers (*e.g.*, cross attention [6, 2] and hyper attention [64]), enabling fusion between the text sequence \mathbf{t} and visual features \mathbf{v} within the Θ -parameterized LLM:

$$\mathbf{H}_0 = \mathbf{t}, \quad \mathbf{H}_{\ell+1} = \Theta_\ell(\Phi_\ell(\mathbf{v}, \mathbf{H}_\ell)) \quad (1)$$

where \mathbf{H}_ℓ denotes the hidden states at layer ℓ , $\Phi_\ell(\cdot, \cdot)$ represents the inserted cross-modal interaction module, and $\Theta_\ell(\cdot)$ denotes the ℓ -th layer of the LLM. While this method ensures direct multimodal

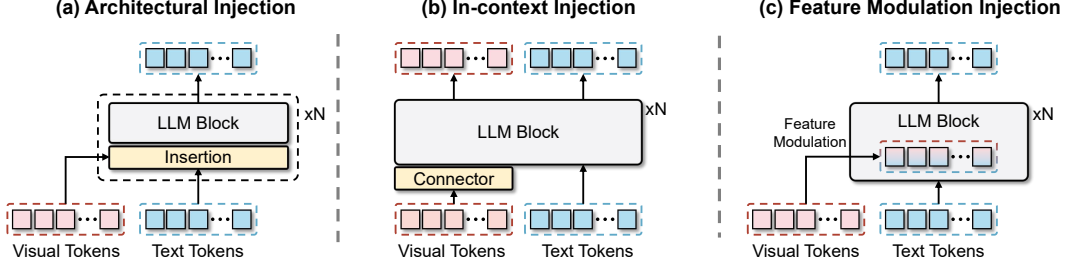


Figure 2: **Comparisons of various vision integration techniques for LLMs.** (a) Architectural injection: additional layers are inserted into LLM for cross-modal interaction; (b) In-context injection: visual tokens are concatenated before the text sequence as the initial context. (c) Feature modulation injection (Ours): the internal hidden states are modulated by the vision-guided affine transformation.

alignment, it comes at the cost of architectural disruption, requiring extensive modifications to the pretrained LLMs. Such modifications compromise the model’s linguistic priors, potentially degrading the generative capabilities in both multimodal and language-only contexts.

In-context Injection. As illustrated in Figure 2b, this approach involves mapping visual features v into the LLM’s semantic space via a vision-language connector [29, 27, 40, 39] and appending them as a visual prefix before the text sequence t :

$$\mathbf{H}_0 = [v; t], \quad \mathbf{H}_{\ell+1} = \Theta_{\ell}(\mathbf{H}_{\ell}) \quad (2)$$

This method allows cross-modal interaction to occur within the LLM’s existing self-attention layers, avoiding explicit structural modifications. However, because self-attention scales quadratically with sequence length [60], the introduction of numerous visual tokens leads to severe computational inefficiencies. This becomes particularly problematic when processing high-resolution images or long video sequences, where the number of visual tokens grows significantly.

To address the inefficiencies of these approaches, we propose feature modulation injection (FMI), as depicted in Figure 2c. Instead of injecting additional layers or expanding sequence length, FMI incorporates visual information directly into the internal hidden states of the LLM via a lightweight modulation mechanism. More details are provided in the following section.

3.2 Feature Modulation Injection.

At the core of FMI is the Layer Normalization (LN) module [7, 68], a ubiquitous and essential component in virtually all mainstream LLM architectures. Given an input text sequence $t = \{t_i\}_{i=1}^T$, a typical LLM block processes t as follows:

$$t \leftarrow t + \mathcal{F}_{att}(\text{LN}_1(t)) \quad (3)$$

$$t \leftarrow t + \mathcal{F}_{ffn}(\text{LN}_2(t)) \quad (4)$$

Here, \mathcal{F}_{att} and \mathcal{F}_{ffn} denote the self-attention and feed-forward sub-layers, respectively. The LN module normalizes the input features via:

$$\text{LN}(t) = \alpha \odot \frac{t - \mu}{\sigma} + \beta = \alpha \odot \hat{t} + \beta \quad (5)$$

where μ and σ are the mean and standard deviation of t , and α, β are learnable affine parameters that control the scaling and shifting of the normalized features. Inspired by this, we propose to *link the learning of affine parameters to visual features*, thereby making the modulation of internal text representations within LN explicitly vision-conditioned. Specifically, we define the following Vision-Infused Layer Normalization (ViLN):

$$\text{ViLN}(t, v) = (\alpha + \Delta\alpha_v) \odot \hat{t} + (\beta + \Delta\beta_v), \quad (6)$$

Here, $\Delta\alpha_v$ and $\Delta\beta_v$ are vision-guided modulation parameters that adaptively adjust the original affine parameters α and β in LLM based on visual context. They are dynamically regressed from visual features v through a token-wise conditioning module, which will be detailed later.

Overall, FMI transforms visual information into affine parameters that directly adjust the LLM’s internal hidden states via *multiplicative* and *additive* operations. This enables a direct and efficient fusion of vision information at the feature level, eliminating the need for lengthy visual token sequences or additional cross-modal interaction modules.

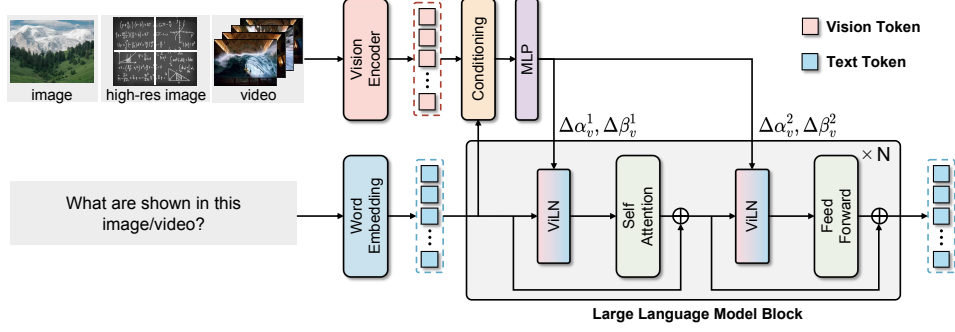


Figure 3: **An illustrative diagram of the overall model architecture.** For a LLM block equipped with ViLN, visual and textual features are fed into the conditioning module to obtain token-wise visual conditions. Through a lightweight MLP, these conditions are then transformed into scale and shift parameters, which modulate the internal linguistic features of the LLM.

3.3 LaVi: A Highly Efficient LVLM

The overall architecture of LaVi is illustrated in Figure 3. After replacing the internal LN of the LLM with ViLN, LaVi leverages a conditioning module to generate token-wise affine parameters from visual features v , comprising two sets that are applied before the self-attention sublayers, respectively:

$$[\Delta\alpha_v^1, \Delta\beta_v^1, \Delta\alpha_v^2, \Delta\beta_v^2] = \text{Swi}(\text{Cond}(t, v))\mathbf{W} + \mathbf{b} \quad (7)$$

Here, $\text{Swi}(\cdot)$ denotes the Swish activation function [51], while \mathbf{W} and \mathbf{b} are learnable projection weights and bias, respectively. This projection is zero-initialized to ensure that the vision-conditioned *deltas* are initially zero, so that the forward pass exactly replicates the original LLM behavior—thereby facilitating stable adaptation and linguistic priors preservation during early training.

The conditioning function $\text{Cond}(\cdot)$ is responsible for aggregating visual context relevant to each token in the text sequence t . The design of this function is highly flexible. In this paper, we explore three alternative instantiations:

MLP-based Conditioning. Inspired by MLP-Mixer [56], we design two sequential MLPs to aggregate visual context. Given a text token t_i , we concatenate it with visual features v , then transpose the sequence $[t_i; v]$ to interchange token and channel dimensions. A token-mixing MLP integrates information across tokens, and after transposing back, a channel-mixing MLP blends features across dimensions. The vision-aware embedding for t_i is then extracted at original position:

$$\text{Cond}_{mlp}(t_i, v) = \left[\text{MLP}_{channel} \left(\left(\text{MLP}_{token} \left([t_i; v]^\top \right) \right)^\top \right) \right]_{t_i} \quad (8)$$

Conv-based Conditioning. Inspired by ConvMixer [59], we treat the concatenated sequence $[t_i; v]$ as a 1-D signal along the token dimension. We first apply a depth-wise convolution followed by an activation σ to mix information between t_i and visual features v . Subsequently, a point-wise convolution is utilized to integrate these features across the embedding dimension. The resulting representation at the token position corresponding to t_i provides the vision-aware embedding:

$$\text{Cond}_{conv}(t_i, v) = \left[\text{Conv}_{point} \left(\sigma \left(\text{Conv}_{depth} \left([t_i; v] \right) \right) \right) \right]_{t_i} \quad (9)$$

Attention-based Conditioning. We introduce a cross-attention module, where text token t_i is used as the query, while visual tokens v serve as keys and values. Through the attention mechanism, we directly aggregate relevant visual context to produce the vision-aware representation for t_i :

$$\text{Cond}_{attn}(t_i, v) = \text{Attention}(t_i \mathbf{W}_Q, v \mathbf{W}_K, v \mathbf{W}_V) \quad (10)$$

We provide further implementation details for the three paradigms in the Appendix. By default, we adopt the attention-based approach due to its simplicity and effectiveness. In Section 4.3, we provide a comparative analysis of each conditioning function, demonstrating that all approaches provide robust multimodal integration with minimal computational overhead.

Scalable Visual Input Support. LaVi flexibly accommodates more complex visual inputs—such as high-resolution images and videos—while requiring only minimal structural modifications, making it

Table 1: **Performance on 9 image-based benchmarks**, including VQAv2, GQA, VisWiz, ScienceQA, TextVQA, POPE, MME^P, MMBench and SEED^I. For MME^P, the scores are presented as percentages. Along with efficiency and accuracy, we also report the LLM backbone for each baseline.

Method	LLM	Efficiency		Performance									
		FLOPs	Latency	VQA ^{v2}	GQA	VisWiz	SciQA	VQA ^T	POPE	MME ^P	MMB	SEED ^I	Avg.
<i>Baselines with $\leq 2B$ parameters scale</i>													
MoE-LLaVA [36]	StableLM-1.6B	3.8	206.4	76.0	60.4	37.2	62.6	47.8	84.3	65.0	59.4	–	–
MobileVLM-V2 [18]	MLLaMA-1.4B	4.3	214.9	–	59.3	–	66.7	52.1	84.3	65.1	57.7	–	–
SPHINX-tiny [38]	TLLaMA-1.1B	4.1	212.3	74.7	58.0	49.2	21.5	57.8	82.2	63.1	56.6	25.2	54.3
LLaVA-OV [27]	Qwen2-0.5B	7.8	228.0	78.5	58.0	51.4	67.2	65.9	86.0	61.9	52.1	65.5	65.2
<i>Baselines with $\leq 8B$ parameters scale</i>													
Qwen-VL-Chat [8]	Qwen-7B	8.2	239.4	78.2	57.5	38.9	68.2	61.5	–	74.4	60.6	65.4	–
mPLUG-Owl2 [65]	LLaMA2-7B	9.3	278.6	79.4	56.1	54.5	68.7	54.3	–	72.5	64.5	57.8	–
Cambrian-1 [57]	LLaMA3-8B	18.6	393.7	–	64.6	–	80.4	71.7	–	77.4	75.9	74.7	–
LLaVA-v1.5 [39]	Vicuna-7B	8.4	254.4	78.5	62.0	50.0	66.8	58.2	85.9	75.5	64.3	66.1	67.5
LLaVA-v1.6 [40]	Vicuna-7B	32.9	502.4	81.8	64.2	57.6	70.1	64.9	86.5	76.0	67.4	70.2	71.0
LLaVA-OV [27]	Qwen2-7B	60.4	612.5	84.5	62.2	53.0	96.0	76.1	87.4	79.0	80.8	75.4	77.2
<i>Ours</i>													
LaVi-Image	Vicuna-7B	0.6	110.8	79.6	63.0	52.9	67.8	58.4	86.9	75.2	64.8	67.5	68.5
Δ compare to LLaVA-v1.5		7.1%	43.6%	+1.1	+1.0	+2.9	+1.0	+0.2	+1.0	-0.3	+0.5	+1.4	+1.0
LaVi-Image (HD)	Vicuna-7B	1.7	148.6	81.4	63.7	57.8	71.7	64.3	87.0	77.5	68.1	71.6	71.5
Δ compare to LLaVA-v1.6		5.2%	29.6%	-0.4	-0.5	+0.2	+1.6	-0.6	+0.5	+1.5	+0.7	+1.4	+0.5
LaVi	Qwen2-7B	3.6	198.1	84.0	65.0	53.8	95.4	77.0	87.1	80.9	79.3	76.9	77.7
Δ compare to LLaVA-OV		6.0%	32.3%	-0.5	+2.8	+0.8	-0.6	+0.9	-0.3	+1.9	-1.5	+1.5	+0.5

broadly applicable across diverse vision-language scenarios. Specifically, for high-resolution images, we adopt a tiling strategy, where the image is divided into non-overlapping tiles compatible with the native input size of the vision encoder. Each tile is independently encoded, and the resulting visual tokens are concatenated along the sequence dimension. For videos, we uniformly sample k frames. Each frame is encoded by the vision encoder and undergoes 2×2 adaptive pooling. The resulting frame features are concatenated sequentially, with shared temporal position encoding applied to each frame’s tokens to capture temporal dynamics.

4 Experiments

4.1 Experimental Settings

Implementation Details. We sequentially train three models to investigate the potential and scalability of the proposed architecture. We begin with LaVi-Image, which mirrors the configuration of LLaVA-v1.5 [39], using the CLIP ViT-L/336px [49] as the vision encoder and Vicuna-v1.5-7B [17] as the LLM backbone. For high-resolution scalability, we incorporate a dynamic high-resolution mechanism adopted in LLaVA-v1.6 [40] for fair comparison, resulting in LaVi-Image (HD). Furthermore, to explore the full potential of the proposed approach, we extend it to an advanced version, LaVi, which is capable of handling both image and video understanding. For LaVi, in line with LLaVA-OneVision [27], we replace the vision encoder with the SigLIP ViT-SO400M/384px [67] and use Qwen2-7B-Instruct [63] as the LLM backbone. For all three variants, we uniformly select 25% of the layers in the LLMs and replace their original LN modules with ViLN, upon which FMI is applied. We adopt the attention-based conditioning as the default method. For image inputs, the full outputs of the vision encoder are utilized for the vision conditioning. For video inputs, 32 frames are uniformly sampled. All experiments are conducted on 16 NVIDIA A100 GPUs, with the training hyperparameters detailed in the Appendix.

Training Data. (1) Pre-training Datasets. We train all three LaVi variants using publicly available images from CC12M [10]. Following the pre-processing pipeline outlined in [49], we retain only samples with resolutions exceeding 448×448 , resulting in a curated subset of 8M samples. (2) Supervised Fine-tuning Datasets. For LaVi-Image, we leverage the instruction datasets corresponding to LLaVA-v1.5 [39], *i.e.*, LLaVA-665K. For LaVi-Image (HD), we leverage the instruction datasets corresponding to LLaVA-v1.6 [40], *i.e.*, LLaVA-760K. For LaVi, we leverage the instruction data from LLaVA-OneVision [27]. For further details, please refer to the Appendix.

Evaluation Benchmarks and Metrics. We evaluate LaVi on both image and video understanding tasks, including 9 image benchmarks and 6 video benchmarks. For evaluation metrics, we report two categories: *computational efficiency* and *benchmark accuracy*. Specifically, computational efficiency includes FLOPs (T) and latency (ms). Further details could be found in the Appendix.

Table 2: **Performance on 6 video-based benchmarks**, including EgoSchema, MLVU, VideoMME, MVBench, CinePile and Video-ChatGPT. Along with computational efficiency and accuracy metrics, we also report the number of sampled frames for each video.

Method	#Frames	Efficiency		Performance					
		FLOPs	Latency	EgoSchema	MLVU	VideoMME	MVBench	CinePile	Video-ChatGPT
Video-LLaVA [37]	8	32.6	488.6	38.4	47.3	39.9	43.1	25.7	2.84
ShareGPT4Video [12]	16	39.2	502.7	–	46.4	43.6	51.2	–	–
VideoLLaMA2 [16]	16	27.3	465.5	51.7	48.5	46.6	54.6	44.6	–
LongVA [71]	32	84.5	742.2	–	–	51.8	–	41.0	3.17
LLaVA-NeXT-Video [40]	32	89.6	775.4	43.9	–	33.7	46.5	–	–
LLaVA-OV [27]	32	129.6	1215.6	60.1	64.7	58.2	–	49.3	3.49
LLaMA-VID [34]	1fps	182.1	2174.3	38.5	33.2	25.9	41.9	–	2.88
LaVi (Ours)	8	4.2	217.0	51.8	54.2	49.4	51.8	45.6	3.03
LaVi (Ours)	16	8.9	272.3	55.5	58.5	54.0	54.3	50.3	3.14
LaVi (Ours)	32	18.6	401.5	58.4	62.3	57.3	56.5	54.0	3.23

4.2 Evaluation Results

Image Understanding Evaluation. We compare LaVi with baseline models across 9 benchmarks to assess its efficiency and performance, with results presented in Table 1. LaVi strikes a remarkable balance between computational efficiency and performance when compared with all baseline models. The three LaVi variants—LaVi-Image, LaVi-Image (HD), and LaVi—are compared against LLaVA-v1.5, LLaVA-v1.6, and LLaVA-OV, respectively. Compared to their counterparts, they achieve reductions of 14.0×, 19.4×, and 16.8× in FLOPs cost. Despite substantial reductions in computational overhead, the three variants achieve 1.0%, 0.5%, and 0.5% average accuracy improvements across all benchmarks, respectively. These results underscore the superior cross-modal interaction efficiency of FMI compared to existing integration strategies. A more comprehensive comparison of the three strategies is provided in Table 4 of Section 4.3 for further reference.

Video Understanding Evaluation. We compare LaVi with advanced video baseline models across 6 widely used benchmarks. To conduct a more comprehensive comparative analysis, in addition to the default setting of 32 frames, we further train two versions utilizing 8 and 16 frames, respectively. The results are presented in Table 2. The superiority of LaVi is strikingly clear. It demonstrates significant computational efficiency, achieving a 6× to 7× reduction in FLOPs compared to baseline models with identical frame counts. Notably, the FLOPs required for the 32-frame LaVi are comparable to half of those needed by the 8-frame Video-LLaVA [37]. LaVi also consistently surpasses or matches the baseline models in performance across all tested frame configurations. We further provide a thorough analysis of the computational overhead associated with frame extension in Section 4.4.

4.3 Ablation Study

In this section, we conduct a comprehensive ablation study of the proposed method. For all experiments in this section, we adopt SigLIP ViT-SO400M [67] as vision encoder and Qwen2-7B-Instruct [63] as LLM backbone. For training data, we uniformly leverage a 4M subset of the pretraining dataset and LLaVA-665K for alignment and SFT, respectively.

Comprehensive Comparison of Integration Techniques. Under identical data and backbone settings, we present a comprehensive comparison of different vision information injection paradigms discussed in Figure 2. For architectural injection, we evaluate two types of inserted modules: cross-attention from Flamingo [6] and hyper-attention from mPLUG-Owl3[64]. For in-context injection, we follow the LLaVA series by concatenating visual features, mapped through a connector, into the text sequence as context. For the proposed feature modulation injection, we evaluate the three instantiations of the module introduced in Section 3.3. The evaluation of these methods covers multiple dimensions, emphasizing computational efficiency and performance on both language-only and vision-language benchmarks. The results in Table 4 demonstrate that FMI achieves a superior balance between efficiency and performance. Specifically, FMI surpasses existing paradigms in both training time and inference overhead. Additionally, we plot the learning curves of the three injection paradigms during the pre-training phase, as illustrated in Figure 4. FMI achieves faster convergence. With the same pre-training dataset, it requires only 1/8 of the training time of in-context injection to achieve comparable performance. Furthermore, compared to current paradigms with lengthy visual contexts or additional inserted layers, FMI preserves better linguistic proficiency, demonstrating significant advantages on all three language-only benchmarks.

Table 4: **Comparison of integration techniques under identical data and backbone settings.** We present the total training hours (Time), the FLOPs during inference, and the accuracy results on three language-only benchmarks and four vision-language tasks.

Architecture	Efficiency		Language Benchmarks				Vision-Language Benchmarks				
	Training Time	FLOPs	MMLU	MBPP	MATH	Avg.	VQA ^T	GQA	MMB	SEED ^I	Avg.
Qwen2-7B-Instruct	–	–	69.3	66.2	47.8	61.1	–	–	–	–	–
Architectural Injection											
Cross Attention	9.8	2.5	64.8	62.4	40.8	56.0	55.8	62.4	71.6	68.0	64.5
Hyper Attention	8.7	2.3	65.3	62.0	41.2	56.2	56.6	61.8	71.8	68.4	64.7
In-context Injection											
Concat	22.0	11.4	66.2	63.6	42.4	57.4	59.0	63.4	72.0	69.2	65.9
Feature Modulation Injection											
MLP-based	5.8	0.8	68.4	66.0	45.2	59.9	58.4	63.0	72.1	68.6	65.5
Conv-based	6.0	0.8	67.7	65.4	44.9	59.3	58.0	62.7	72.4	67.5	65.2
Attention-based	6.6	0.9	68.2	65.6	44.6	59.5	58.7	63.2	72.7	69.5	66.0

Effect of Modulation at Different Sublayers.

Each LLM layer comprises two sublayers: self-attention and feed-forward. We first investigate the impact of applying ViLN at the sublayer level. Results are detailed in Table 3. Disabling ViLN from either sublayer results in a performance decrement, notably more pronounced when removed from the self-attention sublayer. This observation likely stems from the self-attention sublayer’s pivotal role in handling interactions between tokens, having a more substantial influence on the efficacy of cross-modal interactions.

Effect of Modulation Parameter.

ViLN involves two vision-conditioned affine parameters $\Delta\alpha_v$ and $\Delta\beta_v$, which adaptively perform scaling and shifting operations on the internal hidden states. We present an ablation study of each affine parameter, with findings detailed in Table 5. The results indicate that each parameter positively impacts the overall performance, and the gains attributed to each parameter are comparable. It demonstrates that both additive and multiplicative operations hold similar importance for the effective integration of visual information.

Effect of Modulation Frequency.

We investigate the effect of modulation frequency, defined as the proportion of layers within the LLM that apply ViLN. Specifically, we vary this frequency from 12.5% to 100% and report the corresponding results in Table 6. Notably, applying ViLN to 25% of the layers achieves the best average performance across benchmarks, which suggests that a moderate frequency is sufficient to effectively inject visual context, while higher frequencies may not lead to further gains.

Effect of Modulation Location.

We further study the effect of modulation location by fixing the modulation frequency at 25% and varying the specific layers within the LLM where ViLN is applied. Four strategies are evaluated: shallow (first 25%), deep (last 25%), middle (central 25%), and uniform (evenly spaced). As shown in Table 7, the uniform strategy consistently outperforms the others, indicating that distributing modulation across different depths enables more effective and balanced vision integration.

Table 3: **Effect of modulating different sublayers.**

Injecting visual information into both sublayers yields optimal results.

Attn	FFN	VQA ^T	GQA	MMB	SEED ^I	Avg.
✗	✓	55.4	61.5	71.4	69.2	64.4
✓	✗	57.6	62.4	72.0	67.8	65.0
✓	✓	58.7	63.2	72.7	69.5	66.0

Table 5: **Effect of modulation parameters.**

Each parameter enhances visual information integration through corresponding operation.

$\Delta\alpha_v$	$\Delta\beta_v$	VQA ^T	GQA	MMB	SEED ^I	Avg.
✓	✗	58.1	62.2	70.8	67.7	64.5
✗	✓	59.3	62.7	69.3	66.5	64.5
✓	✓	58.7	63.2	72.7	69.5	66.0

Table 6: **Effect of modulation frequency.**

Applying ViLN at a moderate frequency yields the best average performance.

Frequency	VQA ^T	GQA	MMB	SEED ^I	Avg.
100%	59.1	62.9	71.9	68.2	65.5
50%	58.1	62.5	70.9	69.1	65.2
25%	58.7	63.2	72.7	69.5	66.0
12.5%	57.6	62.2	71.5	67.0	64.6

Table 7: **Effect of modulation location.**

Uniformly distributing ViLN across layers leads to more effective multimodal integration.

Location	VQA ^T	GQA	MMB	SEED ^I	Avg.
shallow	54.7	59.4	69.2	64.5	62.0
middle	56.5	61.6	71.4	67.3	64.2
deep	57.0	60.8	70.1	65.9	63.4
uniform	58.7	63.2	72.7	69.5	66.0

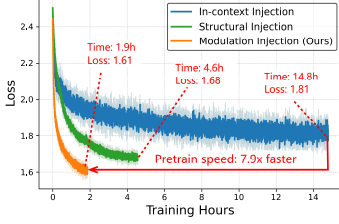


Figure 4: **Training loss of three injection techniques over time.** Our method achieves faster convergence and lower loss.

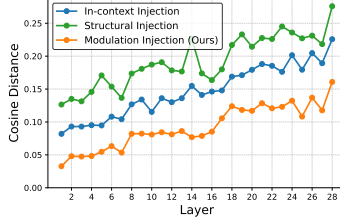


Figure 5: **Feature drifts compared with base LLM.** Our method preserves best linguistic capabilities.

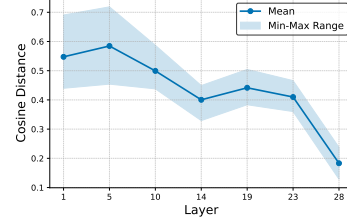


Figure 6: **Features distances before and after ViLN across layers.** Stronger in early layers, while stabilize in deeper layers.

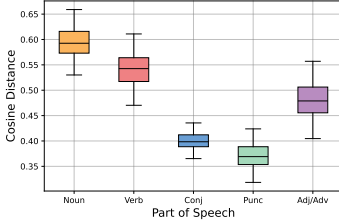


Figure 7: **Modulation influence of LaVi across POS categories.** Semantically rich tokens exhibit stronger modulation influence.

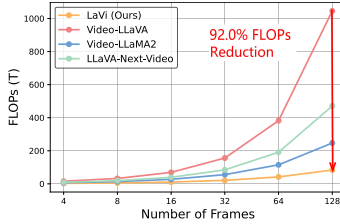


Figure 8: **FLOPs comparison across frame counts.** LaVi achieves significant FLOPs reduction across all frames.

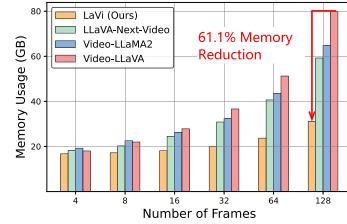


Figure 9: **Memory comparison across frame counts.** LaVi achieves significant Memory reduction across all frames.

4.4 Visualization and Analysis

Effective Preservation of Linguistic Capabilities. For the baselines compared in Table 4, we measure the cosine distance between their hidden states and those of the original base LLM (*i.e.*, Qwen2-7B-Instruct [63]) on QA samples from a language-only benchmark, MMLU [24]. We plot the layer-wise distances in Figure 5. LaVi exhibits minimal feature drift compared to the base LLM, which directly correlates with performance on language-only benchmarks as reported in Table 4. It visually demonstrates that FMI effectively preserves linguistic capabilities.

Stronger Modulation Influence on Early Layers. For LaVi, we compute the cosine distance between features before and after modulation at each layer as a metric for modulation influence on GQA [25]. Figure 6 shows the average distance (solid line) and the range (shaded area) across tokens. The tokens in early layers undergo significant modulation with notable variance among tokens, while deeper layers show reduced influence and stability. This reflects early layers dynamically establishing cross-modal alignments, while deeper layers refine them into coherent representations.

Stronger Modulation Influence on Semantically Rich Tokens. In addition to layer-wise influence, we evaluate the cosine distances across different token types, specifically part-of-speech (POS) categories: nouns, verbs, conjunctions, adjectives/adverbs, and punctuation. POS tagging is performed using the NLTK toolkit [9]. As illustrated in Figure 7, nouns and verbs exhibit more significant modulation influence compared to conjunctions and punctuation. This is intuitive, as nouns and verbs, which carry richer semantic meaning, are more likely to align with and integrate visual information during cross-modal interactions.

Superior Vision Sequence Scalability. High-resolution images and videos increase visual sequence lengths, leading to higher computation and memory demands. We compare FLOPs and GPU memory usage between LaVi and baseline models [16, 37, 40] as frame counts grow, shown in Figure 8 and 9. LaVi achieves significant computational overhead reduction, saving 92.0% and 61.1% in FLOPs and memory, respectively, at 128 frames compared to Video-LLaVA, while maintaining superior performance on video understanding benchmarks. These results demonstrate LaVi’s exceptional computational scalability over existing paradigms.

5 Conclusion

In this work, we propose a novel internal feature modulation injection paradigm for LVLMs, ensuring minimal structural interference and superior computational scalability by avoiding excessive context expansion. Building on this paradigm, we develop LaVi, a highly efficient LVLM that leverages Vision-Infused Layer Normalization (ViLN) for precise visual-linguistic alignment while drastically reducing computational costs. Compared to LLaVA-style models, LaVi achieves 94.0% FLOP reduction, runs 3.1× faster, and significantly lowers latency, establishing LaVi as a highly efficient alternative for vision-language integration.

References

- [1] Josh Achiam, Steven Adler, Sandhini Agarwal, Lama Ahmad, Ilge Akkaya, Florencia Leoni Aleman, Diogo Almeida, Janko Altschmidt, Sam Altman, Shyamal Anadkat, et al. Gpt-4 technical report. *arXiv preprint arXiv:2303.08774*, 2023.
- [2] Jean-Baptiste Alayrac, Jeff Donahue, Pauline Luc, Antoine Miech, Iain Barr, Yana Hasson, Karel Lenc, Arthur Mensch, Katie Millican, Malcolm Reynolds, Roman Ring, Eliza Rutherford, Serkan Cabi, Tengda Han, Zhitao Gong, Sina Samangooei, Marianne Monteiro, Jacob Menick, Sebastian Borgeaud, Andy Brock, Aida Nematzadeh, Sahand Sharifzadeh, Mikolaj Binkowski, Ricardo Barreira, Oriol Vinyals, Andrew Zisserman, and Karen Simonyan. Flamingo: a visual language model for few-shot learning. *ArXiv*, abs/2204.14198, 2022.
- [3] Peter Anderson, Xiaodong He, Chris Buehler, Damien Teney, Mark Johnson, Stephen Gould, and Lei Zhang. Bottom-up and top-down attention for image captioning and visual question answering. In *Proceedings of the IEEE conference on computer vision and pattern recognition*, pages 6077–6086, 2018.
- [4] AI Anthropic. The claude 3 model family: Opus, sonnet, haiku. *Claude-3 Model Card*, 2024.
- [5] Stanislaw Antol, Aishwarya Agrawal, Jiasen Lu, Margaret Mitchell, Dhruv Batra, C Lawrence Zitnick, and Devi Parikh. Vqa: Visual question answering. In *Proceedings of the IEEE international conference on computer vision*, pages 2425–2433, 2015.
- [6] Anas Awadalla, Irena Gao, Josh Gardner, Jack Hessel, Yusuf Hanafy, Wanrong Zhu, Kalyani Marathe, Yonatan Bitton, Samir Gadre, Shiori Sagawa, Jenia Jitsev, Simon Kornblith, Pang Wei Koh, Gabriel Ilharco, Mitchell Wortsman, and Ludwig Schmidt. Openflamingo: An open-source framework for training large autoregressive vision-language models. *arXiv preprint arXiv:2308.01390*, 2023.
- [7] Jimmy Lei Ba. Layer normalization. *arXiv preprint arXiv:1607.06450*, 2016.
- [8] Jinze Bai, Shuai Bai, Shusheng Yang, Shijie Wang, Sinan Tan, Peng Wang, Junyang Lin, Chang Zhou, and Jingren Zhou. Qwen-vl: A frontier large vision-language model with versatile abilities. *arXiv preprint arXiv:2308.12966*, 2023.
- [9] Steven Bird. Nltk: the natural language toolkit. In *Proceedings of the COLING/ACL 2006 Interactive Presentation Sessions*, pages 69–72, 2006.
- [10] Soravit Changpinyo, Piyush Sharma, Nan Ding, and Radu Soricut. Conceptual 12m: Pushing web-scale image-text pre-training to recognize long-tail visual concepts. In *Proceedings of the IEEE/CVF conference on computer vision and pattern recognition*, pages 3558–3568, 2021.
- [11] Liang Chen, Haozhe Zhao, Tianyu Liu, Shuai Bai, Junyang Lin, Chang Zhou, and Baobao Chang. An image is worth 1/2 tokens after layer 2: Plug-and-play inference acceleration for large vision-language models. In *European Conference on Computer Vision*, pages 19–35. Springer, 2024.
- [12] Lin Chen, Xilin Wei, Jinsong Li, Xiaoyi Dong, Pan Zhang, Yuhang Zang, Zehui Chen, Haodong Duan, Bin Lin, Zhenyu Tang, et al. Sharegpt4video: Improving video understanding and generation with better captions. *arXiv preprint arXiv:2406.04325*, 2024.

- [13] Yen-Chun Chen, Linjie Li, Licheng Yu, Ahmed El Kholy, Faisal Ahmed, Zhe Gan, Yu Cheng, and Jingjing Liu. Uniter: Universal image-text representation learning. In *European conference on computer vision*, pages 104–120. Springer, 2020.
- [14] Zhe Chen, Weiyun Wang, Hao Tian, Shenglong Ye, Zhangwei Gao, Erfei Cui, Wenwen Tong, Kongzhi Hu, Jiapeng Luo, Zheng Ma, et al. How far are we to gpt-4v? closing the gap to commercial multimodal models with open-source suites. *Science China Information Sciences*, 67(12):220101, 2024.
- [15] Zhe Chen, Jiannan Wu, Wenhai Wang, Weijie Su, Guo Chen, Sen Xing, Muyan Zhong, Qinglong Zhang, Xizhou Zhu, Lewei Lu, et al. Internvl: Scaling up vision foundation models and aligning for generic visual-linguistic tasks. In *Proceedings of the IEEE/CVF conference on computer vision and pattern recognition*, pages 24185–24198, 2024.
- [16] Zesen Cheng, Sicong Leng, Hang Zhang, Yifei Xin, Xin Li, Guanzheng Chen, Yongxin Zhu, Wenqi Zhang, Ziyang Luo, Deli Zhao, and Lidong Bing. Videollama 2: Advancing spatial-temporal modeling and audio understanding in video-llms. *arXiv preprint arXiv:2406.07476*, 2024.
- [17] Wei-Lin Chiang, Zhuohan Li, Zi Lin, Ying Sheng, Zhanghao Wu, Hao Zhang, Lianmin Zheng, Siyuan Zhuang, Yonghao Zhuang, Joseph E. Gonzalez, Ion Stoica, and Eric P. Xing. Vicuna: An open-source chatbot impressing gpt-4 with 90%* chatgpt quality, March 2023.
- [18] Xiangxiang Chu, Limeng Qiao, Xinyu Zhang, Shuang Xu, Fei Wei, Yang Yang, Xiaofei Sun, Yiming Hu, Xinyang Lin, Bo Zhang, et al. Mobilevlm v2: Faster and stronger baseline for vision language model. *arXiv preprint arXiv:2402.03766*, 2024.
- [19] Chaoyou Fu, Peixian Chen, Yunhang Shen, Yulei Qin, Mengdan Zhang, Xu Lin, Jinrui Yang, Xiawu Zheng, Ke Li, Xing Sun, et al. Mme: A comprehensive evaluation benchmark for multimodal large language models. *arXiv preprint arXiv:2306.13394*, 2023.
- [20] Chaoyou Fu, Yuhan Dai, Yongdong Luo, Lei Li, Shuhuai Ren, Renrui Zhang, Zihan Wang, Chenyu Zhou, Yunhang Shen, Mengdan Zhang, et al. Video-mme: The first-ever comprehensive evaluation benchmark of multi-modal llms in video analysis. *arXiv preprint arXiv:2405.21075*, 2024.
- [21] Yash Goyal, Tejas Khot, Douglas Summers-Stay, Dhruv Batra, and Devi Parikh. Making the v in vqa matter: Elevating the role of image understanding in visual question answering. In *Proceedings of the IEEE conference on computer vision and pattern recognition*, pages 6904–6913, 2017.
- [22] Zonghao Guo, Ruyi Xu, Yuan Yao, Junbo Cui, Zanlin Ni, Chunjiang Ge, Tat-Seng Chua, Zhiyuan Liu, and Gao Huang. Llava-uhd: an lmm perceiving any aspect ratio and high-resolution images. In *European Conference on Computer Vision*, pages 390–406. Springer, 2024.
- [23] Danna Gurari, Qing Li, Abigale J Stangl, Anhong Guo, Chi Lin, Kristen Grauman, Jiebo Luo, and Jeffrey P Bigham. Vizwiz grand challenge: Answering visual questions from blind people. In *Proceedings of the IEEE conference on computer vision and pattern recognition*, pages 3608–3617, 2018.
- [24] Dan Hendrycks, Collin Burns, Steven Basart, Andy Zou, Mantas Mazeika, Dawn Song, and Jacob Steinhardt. Measuring massive multitask language understanding. *arXiv preprint arXiv:2009.03300*, 2020.
- [25] Drew A Hudson and Christopher D Manning. Gqa: A new dataset for real-world visual reasoning and compositional question answering. In *Proceedings of the IEEE/CVF conference on computer vision and pattern recognition*, pages 6700–6709, 2019.
- [26] Allan Jabri, Armand Joulin, and Laurens Van Der Maaten. Revisiting visual question answering baselines. In *European conference on computer vision*, pages 727–739. Springer, 2016.

- [27] Bo Li, Yuanhan Zhang, Dong Guo, Renrui Zhang, Feng Li, Hao Zhang, Kaichen Zhang, Peiyuan Zhang, Yanwei Li, Ziwei Liu, et al. Llava-onevision: Easy visual task transfer. *arXiv preprint arXiv:2408.03326*, 2024.
- [28] Bohao Li, Yuying Ge, Yixiao Ge, Guangzhi Wang, Rui Wang, Ruimao Zhang, and Ying Shan. Seed-bench: Benchmarking multimodal large language models. In *Proceedings of the IEEE/CVF Conference on Computer Vision and Pattern Recognition*, pages 13299–13308, 2024.
- [29] Junnan Li, Dongxu Li, Silvio Savarese, and Steven Hoi. Blip-2: Bootstrapping language-image pre-training with frozen image encoders and large language models. In *International conference on machine learning*, pages 19730–19742. PMLR, 2023.
- [30] Junnan Li, Dongxu Li, Caiming Xiong, and Steven Hoi. Blip: Bootstrapping language-image pre-training for unified vision-language understanding and generation. In *International conference on machine learning*, pages 12888–12900. PMLR, 2022.
- [31] Junnan Li, Ramprasaath Selvaraju, Akhilesh Gotmare, Shafiq Joty, Caiming Xiong, and Steven Chu Hong Hoi. Align before fuse: Vision and language representation learning with momentum distillation. *Advances in neural information processing systems*, 34:9694–9705, 2021.
- [32] KunChang Li, Yanan He, Yi Wang, Yizhuo Li, Wenhai Wang, Ping Luo, Yali Wang, Limin Wang, and Yu Qiao. Videochat: Chat-centric video understanding, 2023.
- [33] Kunchang Li, Yali Wang, Yanan He, Yizhuo Li, Yi Wang, Yi Liu, Zun Wang, Jilan Xu, Guo Chen, Ping Luo, et al. Mvbench: A comprehensive multi-modal video understanding benchmark. In *Proceedings of the IEEE/CVF Conference on Computer Vision and Pattern Recognition*, pages 22195–22206, 2024.
- [34] Yanwei Li, Chengyao Wang, and Jiaya Jia. Llama-vid: An image is worth 2 tokens in large language models. In *European Conference on Computer Vision*, pages 323–340. Springer, 2024.
- [35] Yifan Li, Yifan Du, Kun Zhou, Jinpeng Wang, Wayne Xin Zhao, and Ji-Rong Wen. Evaluating object hallucination in large vision-language models. *arXiv preprint arXiv:2305.10355*, 2023.
- [36] Bin Lin, Zhenyu Tang, Yang Ye, Jiayi Cui, Bin Zhu, Peng Jin, Junwu Zhang, Munan Ning, and Li Yuan. Moe-llava: Mixture of experts for large vision-language models. *arXiv preprint arXiv:2401.15947*, 2024.
- [37] Bin Lin, Bin Zhu, Yang Ye, Munan Ning, Peng Jin, and Li Yuan. Video-llava: Learning united visual representation by alignment before projection. *arXiv preprint arXiv:2311.10122*, 2023.
- [38] Dongyang Liu, Renrui Zhang, Longtian Qiu, Siyuan Huang, Weifeng Lin, Shitian Zhao, Shijie Geng, Ziyi Lin, Peng Jin, Kaipeng Zhang, et al. Sphinx-x: Scaling data and parameters for a family of multi-modal large language models. *arXiv preprint arXiv:2402.05935*, 2024.
- [39] Haotian Liu, Chunyuan Li, Yuheng Li, and Yong Jae Lee. Improved baselines with visual instruction tuning, 2023.
- [40] Haotian Liu, Chunyuan Li, Yuheng Li, Bo Li, Yuanhan Zhang, Sheng Shen, and Yong Jae Lee. Llava-next: Improved reasoning, ocr, and world knowledge, January 2024.
- [41] Haotian Liu, Chunyuan Li, Qingyang Wu, and Yong Jae Lee. Visual instruction tuning. *Advances in neural information processing systems*, 36:34892–34916, 2023.
- [42] Yuan Liu, Haodong Duan, Yuanhan Zhang, Bo Li, Songyang Zhang, Wangbo Zhao, Yike Yuan, Jiaqi Wang, Conghui He, Ziwei Liu, et al. Mmbench: Is your multi-modal model an all-around player? In *European conference on computer vision*, pages 216–233. Springer, 2024.
- [43] Jiasen Lu, Dhruv Batra, Devi Parikh, and Stefan Lee. Vilbert: Pretraining task-agnostic visiolinguistic representations for vision-and-language tasks. *arXiv preprint arXiv:1908.02265*, 2019.

- [44] Pan Lu, Swaroop Mishra, Tanglin Xia, Liang Qiu, Kai-Wei Chang, Song-Chun Zhu, Oyvind Tafjord, Peter Clark, and Ashwin Kalyan. Learn to explain: Multimodal reasoning via thought chains for science question answering. *Advances in Neural Information Processing Systems*, 35:2507–2521, 2022.
- [45] Gen Luo, Xue Yang, Wenhan Dou, Zhaokai Wang, Jifeng Dai, Yu Qiao, and Xizhou Zhu. Mono-intervl: Pushing the boundaries of monolithic multimodal large language models with endogenous visual pre-training. *arXiv preprint arXiv:2410.08202*, 2024.
- [46] Muhammad Maaz, Hanoona Rasheed, Salman Khan, and Fahad Shahbaz Khan. Video-chatgpt: Towards detailed video understanding via large vision and language models. *arXiv preprint arXiv:2306.05424*, 2023.
- [47] Karttikeya Mangalam, Raiymbek Akshulakov, and Jitendra Malik. Egoschema: A diagnostic benchmark for very long-form video language understanding. *Advances in Neural Information Processing Systems*, 36:46212–46244, 2023.
- [48] AI Meta. Llama 3.2: Revolutionizing edge ai and vision with open, customizable models. *Meta AI Blog*. Retrieved December, 20:2024, 2024.
- [49] Alec Radford, Jong Wook Kim, Chris Hallacy, Aditya Ramesh, Gabriel Goh, Sandhini Agarwal, Girish Sastry, Amanda Askell, Pamela Mishkin, Jack Clark, et al. Learning transferable visual models from natural language supervision. In *International conference on machine learning*, pages 8748–8763. PMLR, 2021.
- [50] Alec Radford, Jeffrey Wu, Rewon Child, David Luan, Dario Amodei, Ilya Sutskever, et al. Language models are unsupervised multitask learners. *OpenAI blog*, 2019.
- [51] Prajit Ramachandran, Barret Zoph, and Quoc V Le. Searching for activation functions. *arXiv preprint arXiv:1710.05941*, 2017.
- [52] Ruchit Rawal, Khalid Saifullah, Miquel Farré, Ronen Basri, David Jacobs, Gowthami Somepalli, and Tom Goldstein. Cinepile: A long video question answering dataset and benchmark. *arXiv preprint arXiv:2405.08813*, 2024.
- [53] Amanpreet Singh, Vivek Natarajan, Meet Shah, Yu Jiang, Xinlei Chen, Dhruv Batra, Devi Parikh, and Marcus Rohrbach. Towards vqa models that can read. In *Proceedings of the IEEE/CVF conference on computer vision and pattern recognition*, pages 8317–8326, 2019.
- [54] DeepSpeed Team. Flops profiler, 2025. Accessed: 2025-02-11.
- [55] Gemini Team, Rohan Anil, Sebastian Borgeaud, Jean-Baptiste Alayrac, Jiahui Yu, Radu Soricut, Johan Schalkwyk, Andrew M Dai, Anja Hauth, Katie Millican, et al. Gemini: a family of highly capable multimodal models. *arXiv preprint arXiv:2312.11805*, 2023.
- [56] Ilya O Tolstikhin, Neil Houlsby, Alexander Kolesnikov, Lucas Beyer, Xiaohua Zhai, Thomas Unterthiner, Jessica Yung, Andreas Steiner, Daniel Keysers, Jakob Uszkoreit, et al. Mlp-mixer: An all-mlp architecture for vision. *Advances in neural information processing systems*, 34:24261–24272, 2021.
- [57] Shengbang Tong, Ellis Brown, Penghao Wu, Sanghyun Woo, Manoj Middepogu, Sai Charitha Akula, Jihan Yang, Shusheng Yang, Adithya Iyer, Xichen Pan, et al. Cambrian-1: A fully open, vision-centric exploration of multimodal llms. *arXiv preprint arXiv:2406.16860*, 2024.
- [58] Hugo Touvron, Louis Martin, Kevin Stone, Peter Albert, Amjad Almahairi, Yasmine Babaei, Nikolay Bashlykov, Soumya Batra, Prajjwal Bhargava, Shruti Bhosale, et al. Llama 2: Open foundation and fine-tuned chat models. *arXiv preprint arXiv:2307.09288*, 2023.
- [59] Asher Trockman and J Zico Kolter. Patches are all you need? *arXiv preprint arXiv:2201.09792*, 2022.
- [60] Ashish Vaswani, Noam Shazeer, Niki Parmar, Jakob Uszkoreit, Llion Jones, Aidan N Gomez, Łukasz Kaiser, and Illia Polosukhin. Attention is all you need. *Advances in neural information processing systems*, 30, 2017.

- [61] Zhongwei Wan, Ziang Wu, Che Liu, Jinfa Huang, Zhihong Zhu, Peng Jin, Longyue Wang, and Li Yuan. Look-m: Look-once optimization in kv cache for efficient multimodal long-context inference. *arXiv preprint arXiv:2406.18139*, 2024.
- [62] Weihang Wang, Qingsong Lv, Wenmeng Yu, Wenyi Hong, Ji Qi, Yan Wang, Junhui Ji, Zhuoyi Yang, Lei Zhao, Song XiXuan, et al. CogVLM: Visual expert for pretrained language models. *Advances in Neural Information Processing Systems*, 37:121475–121499, 2025.
- [63] An Yang, Baosong Yang, Binyuan Hui, Bo Zheng, Bowen Yu, Chang Zhou, Chengpeng Li, Chengyuan Li, Dayiheng Liu, Fei Huang, et al. Qwen2 technical report. *arXiv preprint arXiv:2407.10671*, 2024.
- [64] Jiabo Ye, Haiyang Xu, Haowei Liu, Anwen Hu, Ming Yan, Qi Qian, Ji Zhang, Fei Huang, and Jingren Zhou. mplug-owl3: Towards long image-sequence understanding in multi-modal large language models. In *The Thirteenth International Conference on Learning Representations*, 2024.
- [65] Qinghao Ye, Haiyang Xu, Jiabo Ye, Ming Yan, Anwen Hu, Haowei Liu, Qi Qian, Ji Zhang, and Fei Huang. mplug-owl2: Revolutionizing multi-modal large language model with modality collaboration. In *Proceedings of the IEEE/CVF Conference on Computer Vision and Pattern Recognition*, pages 13040–13051, 2024.
- [66] Jiahui Yu, Zirui Wang, Vijay Vasudevan, Legg Yeung, Mojtaba Seyedhosseini, and Yonghui Wu. Coca: Contrastive captioners are image-text foundation models. *arXiv preprint arXiv:2205.01917*, 2022.
- [67] Xiaohua Zhai, Basil Mustafa, Alexander Kolesnikov, and Lucas Beyer. Sigmoid loss for language image pre-training. In *Proceedings of the IEEE/CVF International Conference on Computer Vision*, pages 11975–11986, 2023.
- [68] Biao Zhang and Rico Sennrich. Root mean square layer normalization. *Advances in Neural Information Processing Systems*, 32, 2019.
- [69] Hang Zhang, Xin Li, and Lidong Bing. Video-llama: An instruction-tuned audio-visual language model for video understanding. *arXiv preprint arXiv:2306.02858*, 2023.
- [70] Kaichen Zhang, Bo Li, Peiyuan Zhang, Fanyi Pu, Joshua Adrian Cahyono, Kairui Hu, Shuai Liu, Yuanhan Zhang, Jingkang Yang, Chunyuan Li, et al. Lmms-eval: Reality check on the evaluation of large multimodal models. *arXiv preprint arXiv:2407.12772*, 2024.
- [71] Peiyuan Zhang, Kaichen Zhang, Bo Li, Guangtao Zeng, Jingkang Yang, Yuanhan Zhang, Ziyue Wang, Haoran Tan, Chunyuan Li, and Ziwei Liu. Long context transfer from language to vision. *arXiv preprint arXiv:2406.16852*, 2024.
- [72] Yi-Kai Zhang, Shiyin Lu, Yang Li, Yanqing Ma, Qing-Guo Chen, Zhao Xu, Weihua Luo, Kaifu Zhang, De-Chuan Zhan, and Han-Jia Ye. Wings: Learning multimodal llms without text-only forgetting. *CoRR*, abs/2406.03496, 2024.
- [73] Junjie Zhou, Yan Shu, Bo Zhao, Boya Wu, Shitao Xiao, Xi Yang, Yongping Xiong, Bo Zhang, Tiejun Huang, and Zheng Liu. Mlvu: A comprehensive benchmark for multi-task long video understanding. *arXiv preprint arXiv:2406.04264*, 2024.

A Implementation Details

A.1 Training Details.

The overall training process adopts a two-stage paradigm, initially involving the pretraining of the conditioning module, followed by instruction tuning. Table 8 and Table 9 presents the details of this two-stage training for LaVi. The implementation includes two sets of vision and LLM combinations: CLIP ViT-L/336px [49] + Vicuna [17] or SigLIP ViT-SO400M/384px [67] + Qwen2 [63], aligned with the respective LLaVA configurations. Furthermore, consistent with the settings of LLaVA1.6 and LLaVA-OV, we additionally unfroze the ViT during the SFT phase.

A.2 Benchmark Details.

We conduct a comprehensive evaluation of LaVi, including both image and video understanding benchmarks.

Image-based Benchmarks Following the LLaVA framework [39], we conduct experiments across 9 widely recognized benchmarks, including VQA-v2 (VQA^{v2}) [21], GQA [25], VisWiz [23], ScienceQA-IMG (SciQA) [44], TextVQA (VQA^T) [53], POPE [35], MME [19], MMBench (MMB) [42], SEED-Bench (SEED¹) [28]. These benchmarks span a broad spectrum of visual tasks. Our evaluation protocols are aligned with those established in the LLaVA framework, ensuring fair consistency.

Video-based Benchmarks We conduct experiments across 6 widely recognized benchmarks, including MVBench [33], MLVU [73], EgoSchema [47], VideoMME [20], CinePile [52] and Video-ChatGPT [46]. They cover multiple knowledge dimensions and domain focuses, with video durations ranging from a few seconds to several hours.

A.3 Evaluation Details.

We adopt LMMs-Eval as our evaluation toolkit. For evaluation prompts, we provide a thorough examination of all evaluation benchmarks utilized in this paper in Table 10. For model efficiency, the FLOPs and latency are calculated using the DeepSpeed toolkit [54] on a single A100 GPU without any engineering acceleration techniques.

Table 8: The training details of LaVi based on Vicuna.

Config	Stage I	Stage II
LLM backbone	Vicuna-7B	
ViT backbone	CLIP ViT-L/336px	
Global batch size	1024	256
Batch size per GPU	64	16
Accumulated steps	1	1
DeepSpeed zero stage	2	2
Learning rate	1×10^{-3}	2×10^{-5}
Learning rate schedule	cosine decay	
Warmup ratio	0.03	
Weight decay	0	
Epoch	1	
Optimizer	AdamW	
Precision	bf16	

Table 9: The training details of LaVi base on Qwen.

Config	Stage I	Stage II
LLM backbone	Qwen2-7B	
ViT backbone	SigLIP SO400M/384px	
Global batch size	1024	256
Batch size per GPU	64	16
Accumulated steps	1	1
DeepSpeed zero stage	2	3
Learning rate	1×10^{-3}	1×10^{-5}
Learning rate schedule	cosine decay	
Warmup ratio	0.03	
Weight decay	0	
Epoch	1	
Optimizer	AdamW	
Precision	bf16	

B Conditioning Module

To provide a clearer understanding of the proposed conditioning modules, we present PyTorch-style pseudocode implementations for the three vision-conditioned modulation strategies introduced in Section 3.3. Each variant—MLP-based, Conv-based, and Attention-based—is designed to instantiate the generic conditioning function $\text{Cond}(\cdot)$ used to derive token-wise affine parameters for Vision-Infused Layer Normalization (ViLN). These modules differ in how they aggregate visual context to influence individual text tokens, yet they all share a common design objective: enabling efficient, token-specific vision-language interaction without altering the LLM’s original architecture.

```

1 class MLP_Condition(nn.Module):
2     def __init__(self, embed_dim: int, num_vis_tok: int,
3                 token_exp: int = 4, channel_exp: int = 4):
4         super().__init__()
5         self.L = num_vis_tok + 1 # total tokens (t_i + v)
6         # token-mixing MLP
7         self.mlp_token = nn.Sequential(
8             nn.Linear(self.L, self.L * token_exp),
9             nn.GELU(),
10            nn.Linear(self.L * token_exp, self.L))
11        # channel-mixing MLP
12        self.mlp_channel = nn.Sequential(
13            nn.Linear(embed_dim, embed_dim * channel_exp),
14            nn.GELU(),
15            nn.Linear(embed_dim * channel_exp, embed_dim))
16        def forward(self, t_i: torch.Tensor, v: torch.Tensor) -> torch.
17        Tensor:
18            assert v.size(1) + 1 == self.L, "Unexpected #visual tokens"
19            # concat (B, L, C) where L = 1 + V
20            seq = torch.cat([t_i, v], dim=1) # (B, L, C)
21            # Token mixing
22            x = seq.transpose(1, 2) # (B, C, L) swap token/chan
23            x = self.mlp_token(x)
24            x = x.transpose(1, 2) # back to (B, L, C)
25            # Channel mixing
26            y = self.mlp_channel(x) # (B, L, C)
27            return y[:, 0, :]
28
29 class Conv_Condition(nn.Module):
30     def __init__(self, embed_dim: int, kernel_size: int):
31         super().__init__()
32         pad = kernel_size // 2
33         self.dw = nn.Conv1d(embed_dim, embed_dim, kernel_size,
34                             padding=pad, groups=embed_dim)
35         self.pw = nn.Conv1d(embed_dim, embed_dim, kernel_size=1)
36         self.act = nn.SiLU()
37         def forward(self, t_i: torch.Tensor, v: torch.Tensor) -> torch.
38         Tensor:
39            # concatenate on token dimension, then transpose for Conv1d
40            seq = torch.cat([t_i, v], dim=1).transpose(1, 2) # (B, C, 1+V)
41            # depth-wise conv -> activation -> point-wise conv
42            out = self.pw(self.act(self.dw(seq))).transpose(1, 2) # (B,
43            1+V, C)
44            return out[:, 0, :]
45
46 class Attn_Condition(nn.Module):
47     def __init__(self, C:int, h:int=8):
48         super().__init__()
49         self.q = nn.Linear(C, C, False)
50         self.k = nn.Linear(C, C, False)
51         self.v = nn.Linear(C, C, False)
52         self.o = nn.Linear(C, C, False)
53         def forward(self, t, v): # t:(B,1,C) v:(B,V,C)
54            B = t.size(0)
55            def shp(x):
56                return x.reshape(B, -1, self.h, self.dk).permute(0, 2, 1,
57                3)
58            q, k, val = map(shp, (self.q(t), self.k(v), self.v(v)))
59            attn = (q @ k.transpose(-2, -1)) / math.sqrt(self.dk)
60            ctx = (attn.softmax(-1) @ val).transpose(1, 2).reshape(B, 1,
61            -1)
62            return self.o(ctx).squeeze(1)

```

Figure 10: Implementation of three conditioning modules in PyTorch.

Table 10: **Summary of the evaluation benchmarks.** Prompts are mostly borrowed from LMMs-Eval [70].

Benchmark	Response formatting prompts
POPE [35]	–
GQA [25]	Answer the question using a single word or phrase.
VQA ^{v2} [21]	Answer the question using a single word or phrase.
TextVQA [53]	Answer the question using a single word or phrase.
MME [19]	Answer the question using a single word or phrase.
VisWiz [23]	Answer the question using a single word or phrase. When the provided information is insufficient, respond with Unanswerable’.
SciQA [44]	Answer with the option’s letter from the given choices directly.
MMBench [42]	Answer with the option’s letter from the given choices directly.
SEED-Bench [28]	Answer with the option’s letter from the given choices directly.
MLVU [73]	–
Video-ChatGPT [46]	–
MVBench [33]	Only give the best option.
VideoMME [20]	Answer with the option’s letter from the given choices directly.
EgoSchema [47]	Answer with the option’s letter from the given choices directly.
Cineplie [52]	Answer with the option key (A, B, C, D, E) and nothing else.